American Mineralogist, Volume 81, pages 202–212, 1996

Fluid-absent melting of F-rich phlogopite + rutile + quartz

DEBRA F. DOOLEY* AND ALBERTO E. PATIÑO DOUCE

Department of Geology, University of Georgia, Athens, Georgia 30602, U.S.A.

ABSTRACT

Fluid-absent melting is believed to be an important process in the generation of melts in the lower crust and upper mantle. Breakdown of phlogopite makes H_2O available and thus controls the conditions at which fluid-absent melting occurs. Both F and Ti in biotite have been shown to affect strongly the thermal stability of biotite. To model better the fluid-absent melting of assemblages containing phlogopite, the reaction F-phlogopite + quartz + rutile = enstatite + melt has been studied experimentally. Experiments were performed at 7, 10, and 15 kbar using a natural F-rich phlogopite with a starting composition of F/(F + OH) = 0.43 and Mg/(Mg + Fe) (in molar proportions) = 0.94. Results indicate that the thermal stability of F-rich phlogopite + quartz + rutile is extended by as much as 450 °C relative to the KMASH system and by 300 °C relative to the Ti-free F-KMASH system. Approach to equilibrium in the experiments was assessed by convergence of results of melting and crystallization experiments. Phlogopite compositions from experimental products show that, although F-rich phlogopite incorporates relatively little Ti (2–3 wt% TiO_2), the combination of F and Ti increases the stability of phlogopite to considerably higher temperatures (~300 °C) than that of either component alone. Melts formed by the fluid-absent melting of F-rich phlogopite + quartz + rutile at temperatures > 1000 °C are granitic and strongly peraluminous. The compositions of these melts suggest that the formation of metaluminous to peralkaline A-type granites by fluid-absent melting of halogen-enriched sources is unlikely.

INTRODUCTION

Volatile components present in micas (primarily H_2O and to a lesser extent halogens) facilitate the formation of melts under fluid-absent conditions in both the continental crust and the metasomatically altered mantle (e.g., Wood 1976; Wendlandt and Eggler 1980; Thompson 1982; Bohlen et al. 1983). Breakdown of mica also exerts important controls on processes occurring within subducted oceanic lithosphere (Modreski and Boettcher 1972, 1973; Aoki et al. 1981; Wyllie and Sekine 1982). Because the numerous compositional variations in mica have strong effects on the P, T, and f_{O_2} conditions at which it breaks down, it is important to understand the relationships between composition and stability. Both Ti and F are important components in mica from high-grade metamorphic rocks (e.g., Leelanandam 1969; Dymek 1983; Guidotti 1984; Chacko et al. 1987). However, no systematic work has been done on how these two components interact and, in combination, affect the thermal stability of mica in quartz-saturated assemblages. In particular, the melting relations of Ti- and F-rich phlogopite + quartz are unknown.

Many experimental studies have been performed on the fluid-absent melting behavior of phlogopite in the KMASH system (e.g., Bohlen et al. 1983; Peterson and Newton 1989; Vielzeuf and Clemens 1992) with the assemblages quartz + phlogopite and quartz + phlogopite + sanidine to determine the P and T conditions at which fluid-absent melting occurs. The range in P-T conditions at which phlogopite breaks down to form melt has been tightly constrained by this earlier work. The behavior of phlogopite in the F-bearing system was studied by Peterson et al. (1991), who determined the fluid-absent melting relations of the assemblage F-rich phlogopite + quartz. Fluid-absent melting of an F-rich natural metatonalite containing biotite with Mg′ = 0.31 [Mg′ = Mg/(Mg + Fe) in molar proportions] was studied by Skjerlie and Johnston (1993). The effect of increased F content on mica stability was also studied experimentally by Munoz and Ludington (1977), and the relationship between F content and Al, Fe, and Mg contents in mica was studied by Munoz and Ludington (1974), Petersen et al. (1982), and Valley et al. (1982). Work on Ti substitution mechanisms in phlogopite and biotite includes that of Robert (1976), Monier and Robert (1986), Dymek (1983), and Abrecht and Hewitt (1988), and modeling of the effect of Ti on the thermal stability of phlogopite and biotite was conducted by Trønnes et al. (1985) and Patiño Douce (1993), respectively. Largely as a result of these previous experimental investigations, and through studies of natural as-

* Present address: Department of Geological and Geophysical Sciences, Princeton University, Princeton, New Jersey 08544, U.S.A.

0003–004X/96/0102–0202$05.00

semblages (e.g., Guidotti 1984), it is known that F and Ti substitutions in phlogopite and in biotite independently increase the thermal stabilities of these minerals.

We conducted fluid-absent melting and crystallization experiments with the assemblage F-rich phlogopite + quartz + rutile. These experiments elucidate how temperature and pressure affect F and Ti contents in near end-member phlogopite (Mg′ = 0.94) coexisting with quartz and a Ti-saturating phase and, in turn, suggest how these components affect the upper thermal stability of phlogopite. We also determined the compositions of melts formed during fluid-absent melting of Ti- and F-rich phlogopite + quartz + rutile. This study constitutes an approximation toward clarification of the combined effects of high Ti and F contents on the fluid-absent melting relations of phlogopite and could serve as a model for the behavior of biotite in F- and Ti-rich bulk compositions.

Experimental and analytical procedures

We conducted both melting and crystallization experiments to assess the approach to equilibrium of the experimental results. The starting materials used to perform each kind of experiment are discussed below.

Apparatus

Melting and crystallization experiments were performed at 7, 10, and 15 kbar in a solid-medium piston-cylinder apparatus with 0.5 in. cell assemblies over the temperature interval 1050–1375 °C (Table 1). Pressures were monitored with a Heise gauge yielding an accuracy in nominal sample pressure of ±50 bars. Friction loss was determined to be no more than 0.5 kbar on the basis of the end-member anorthite and albite breakdown reactions [see also Patiño Douce (1995) for additional discussion]. Temperatures were measured using $W_{74}Re_{26}$-$W_{95}Re_5$ thermocouples and controlled with a digital Eurotherm 808 temperature controller. The reported temperatures are believed to be within ±5 °C of the actual sample temperature owing to the small sample size (see below) and proximity of the thermocouple to the capsule (≤1 mm). Cell assemblies consisted of a CaF_2 inner plug containing the encapsulated sample, surrounded by a graphite furnace. The furnace was separated from the NaCl outer bushing by a Pyrex glass sleeve. Initial pressure applied to the assembly was approximately 1 kbar at 25 °C. At temperatures below 675 °C, the pressure was maintained below 7 kbar. Above this T, as the target temperature was approached, pressure was gradually increased. This procedure ensured that the glass sleeve did not shatter before the target conditions were achieved. In most cases, pressure increased during the experiments above the target conditions and had to be monitored and lowered (hot-piston out) throughout the experiment.

Starting materials for melting experiments

Two starting mixtures were used in the melting experiments, both consisting of F-rich phlogopite (Ward's no. 46E6190, from Notre Dame-du-laus, Quebec, Canada), quartz, and rutile. This sample of phlogopite was chosen because it contains a substantial amount of F (3.77 wt%) and a small amount of Fe (Mg′ = 0.94). Brazilian quartz and rutile from Graves Mountain, Georgia, were used as the SiO_2 and TiO_2 phases. Compositions of phlogopite, quartz, and rutile in the starting materials and the modal abundances and bulk compositions of the two starting mixtures are given in Table 2. The chosen modal abundances are similar to those of other experiments performed with the assemblages phlogopite + quartz (Peterson and Newton 1989; Vielzeuf and Clemens 1992) and F-rich phlogopite + quartz (Peterson et al. 1991). Mixture FTi-1 was used to perform a series of preliminary experiments at 10 kbar. However, at 10 kbar and 1263 °C, only a minor amount of rutile was observed. Because the goal of this study was to determine the behavior of F-rich phlogopite under Ti-saturated conditions, a new mixture (FTi-2) was prepared with additional rutile to ensure Ti saturation. This mixture was used for most experiments (Table 1). Estimated H_2O content of the starting materials is ~1 wt%, on the basis of the F-rich starting phlogopite analyses (H_2O determined by charge balance) and of the modal composition of the starting mixtures.

Table 1. Experimental conditions and phase assemblages of experimental products

Expt.	P (kbar)	T (°C)	t (h)	Assemblage
DD56 melting*	7	1038	48	Phl Qtz Rt (Pyx)
DD57 melting	7	1050	42	Phl Qtz Rt Pyx (melt)
DD19 melting**	7	1250	6	Phl Qtz Rt Pyx melt
DD39 crystall.†	7	1250	6	Phl Qtz Rt Pyx melt
DD29 melting	7	1275	4	Phl (Qtz) Rt Pyx melt
DD45 crystall.	7	1275	4	Phl Qtz Rt Pyx melt
DD50 crystall.	7	1290	3.75	(Qtz) Rt Pyx melt
DD27 melting	7	1300	3.5	(Qtz) Rt Pyx melt
DD33 melting	7	1375	0.5	(Rt) Pyx melt
DD40 melting	7	1375	0.5	Rt Pyx melt
DD11 melting**	10	1050	36	Phl Qtz Rt (Pyx)
APD612 melting	10	1075	172	Phl Qtz Rt Pyx (melt)
DD15 melting**	10	1075	52	Phl Qtz Rt Pyx (melt)
DD13 melting**	10	1150	25	Phl Qtz Rt Pyx melt
DD38 crystall.	10	1250	11.5	Phl Qtz Rt Pyx melt
DD14 melting**	10	1263	11	Phl Qtz (Rt) Pyx melt
APD616 melting	10	1275	9	Phl Qtz Rt Pyx melt
DD42 crystall.	10	1275	5	Phl Qtz Rt Pyx melt
DD44 crystall.	10	1290	4.5	Phl Qtz Rt Pyx melt
DD30 melting	10	1300	3.5	Phl (Qtz) Rt Pyx melt
DD34 crystall.	10	1300	3.5	Qtz Rt Pyx melt
DD35 melting	10	1325	3	Qtz Rt Pyx melt
DD31 melting	10	1350	2	(Qtz) (Rt) Pyx melt
DD20 melting**	15	1300	5	Phl Qtz Rt Pyx melt
DD52 melting	15	1300	5	Phl Qtz Rt Pyx melt
DD53 crystall.	15	1300	4.5	Phl Qtz Rt Pyx melt
DD54 crystall.	15	1313	4.5	Phl Qtz Rt Pyx melt
DD48 melting	15	1325	4.5	Qtz Rt Pyx melt
DD51 melting	15	1350	3	Qtz Rt Pyx melt
DD46 crystall.	15	1363	2	Qtz Rt Pyx melt
DD32 melting	15	1400	1.5	Qtz Pyx melt

Note: Abbreviations from Kretz 1983 (Pyx = pyroxene); parentheses indicate minor amount of phase present.

* Melting experiments as described in text.

** Experiments performed with mixture FTi-1 (see text).

† Crystallization experiments as described in text.

TABLE 2. Starting mixtures

	SiO_2	Al_2O_3	TiO_2	FeO	MgO	Na_2O	K_2O	F	Total
				Bulk compositions (wt%)					
Mix FTi-1	68.0	6.6	2.3	1.6	12.9	0.2	5.3	1.9	98.8
Mix FTi-2	66.7	6.5	4.3	1.6	12.6	0.2	5.2	1.9	99.0
				Starting compositions (wt%)					
F-rich Phl	41.3(0.7)	13.0(0.3)	0.6(0.1)	3.1(0.5)	25.3(0.4)	0.4(0.1)	10.3	3.8(0.4)	97.8(1.6)
Qtz	100.8	0.0	0.0	0.0	0.0	0.0	0.0	0.0	100.8
Rt	0.0(0.0)	0.0(0.0)	99.4(0.8)	0.2(0.1)	0.0	—	—	—	99.6(0.8)

Note: Mix FTi-1 consists of 47.0 wt% quartz, 51.0 wt% F-rich phlogopite, and 2.0 wt% rutile. Mix FTi-2 consists of 46.1 wt% quartz, 49.9 wt% F-rich phlogopite, and 4.0 wt% rutile. Numbers in parentheses represent relative uncertainties of the average values (two standard deviations) on the basis of ten analyses of different F-rich phlogopite grains and five analyses of different rutile grains. Phlogopite composition gives a formula of $K_{0.94}Na_{0.05}(Mg_{2.70}Fe_{0.18}Ti_{0.03}Al_{0.06})(Al_{1.04}Si_{2.96})O_{10}(OH)_{1.15}F_{0.85}$. This formula has a value of F/(F + OH) = 0.43. Dashes indicate elements not analyzed.

The phlogopite used in these experiments is similar in F and Mg content [F/(F + OH) = 0.43 vs. 0.54 and Mg′ = 0.94 vs. 1.00, respectively] to the synthetic phlogopite used by Peterson et al. (1991). No F-buffering phase is present in our experiments, but the activity of TiO_2 is buffered if rutile is present.

Starting materials were mixed in an alumina mortar under acetone for 30 min. Approximately 4–6 mg of sample were loaded into $Ag_{25}Pd_{75}$ capsules (3 mm o.d., 0.3 mm wall, 5 mm long) and placed in a 120 °C drying oven for ~24 h to remove any adsorbed water. The capsules were crimped before removal from the oven and immediately sealed by arc-welding. $Ag_{25}Pd_{75}$ capsules were used because the temperatures at which these experiments were performed exceed the melting point of gold. One possible consequence of using these capsules is Fe loss from the sample. Fe contents were determined in capsules from both low- and high-temperature experiments performed at 10 kbar. At 1075 °C, 0.5 wt% FeO (Fe calculated as FeO) was measured in the capsule after 172 h, and at ~1300 °C, 0.8 wt% FeO was measured in the capsule after 28 h. Because the bulk composition is close to the Mg end-member, this Fe loss is not expected to affect the experimental results significantly.

Starting materials for crystallization experiments

Crystallization experiments were performed with the goal of obtaining the same phase assemblages observed in melt-

TABLE 3. Phlogopite compositions

Expt.	DD56	DD57	DD19*	DD39	DD29	DD45	DD11*	DD15*	APD612	DD13*
P (kbar)	7	7	7	7	7	7	10	10	10	10
T (°C)	1038	1050	1250	1250	1275	1275	1050	1075	1075	1150
*n***	4	6	8	3	5	5	8	4	3	7
					wt% oxides					
SiO_2	44.09	43.41	42.56	46.46	43.68	45.13	42.59	42.38	43.26	42.62
Al_2O_3	13.12	13.57	12.68	12.24	11.93	11.32	14.20	13.89	13.70	13.67
TiO_2	0.81	0.70	1.04	2.69	2.27	1.98	0.69	0.93	0.70	0.72
FeO†	2.18	2.06	1.20	0.03	0.01	0.00	1.99	1.67	1.67	0.95
MgO	25.10	25.41	25.31	24.30	27.40	26.20	24.77	23.95	26.02	26.18
Na_2O	0.18	0.12	0.13	0.22	0.09	0.18	0.14	0.23	0.20	0.14
K_2O	9.98	10.43	10.60	9.33	10.19	9.96	10.43	10.49	10.40	10.53
F	5.46	6.44	8.40	7.57	8.16	8.25	5.93	5.78	7.62	7.75
Oxide total	100.92	102.14	101.92	102.85	103.72	103.00	100.74	99.32	103.57	102.56
$-O \equiv F$	2.30	2.71	3.54	3.19	3.43	3.47	2.50	2.43	3.21	3.26
Total	98.62	99.43	98.38	99.66	100.29	99.53	98.24	96.89	100.36	99.30
					Stoichiometries based on O = 11					
Si	3.06	3.02	3.03	3.17	3.00	3.12	2.99	3.01	3.00	2.98
$^{[4]}Al$	0.94	0.98	0.97	0.83	0.97	0.88	1.01	0.99	1.00	1.02
$^{[6]}Al$	0.14	0.13	0.09	0.16	0.00	0.05	0.17	0.18	0.11	0.11
Mg	2.60	2.63	2.68	2.49	2.85	2.71	2.59	2.54	2.69	2.73
Ti	0.04	0.04	0.06	0.14	0.11	0.10	0.04	0.05	0.04	0.04
Fe	0.13	0.12	0.07	0.00	0.01	0.00	0.12	0.10	0.10	0.06
K	0.88	0.93	0.96	0.81	0.88	0.88	0.94	0.95	0.92	0.94
Na	0.02	0.02	0.02	0.03	0.02	0.02	0.01	0.03	0.01	0.02
F	1.20	1.42	1.89	1.64	1.76	1.81	1.32	1.30	1.67	1.72
OH	0.80	0.58	0.11	0.36	0.24	0.19	0.68	0.70	0.33	0.29
F/(F + OH)	0.60	0.71	0.94	0.83	0.88	0.89	0.66	0.65	0.84	0.86

Note: Relative uncertainties of the average values (two standard deviations) are 3% for SiO_2, 4% for MgO and K_2O, 6% for F, 23% for TiO_2, 49% for Na_2O, and 73% for FeO.

* Experiments performed with mixture FTi-1.

** The number of grains analyzed per experiment.

† Total Fe reported as FeO.

ing experiments at the same P-T conditions. Starting materials for the crystallization experiments were prepared by melting the starting crystalline mixture FTi-2 (Table 2) in sealed $Ag_{25}Pd_{75}$ capsules for 30 min at 7 kbar and ≈1375 °C. Prior to their use in the crystallization experiments, the products of these high-temperature melting experiments were examined with the electron microprobe to determine the degree of melting and identify the phases present. Phlogopite and quartz were no longer present at these P-T conditions, but both pyroxene and rutile remained. The amount of melt was estimated to be between 75 and 90%. Portions of the products of these high-T experiments were then used as starting material for crystallization experiments at lower temperatures.

Characterization of experimental products and analytical procedures

The capsules were weighed before and after the experiments. No weight loss was detected in any experimental product. The capsules were also examined optically to ensure that there were no ruptures, which would have allowed CaF_2 contamination from the pressure medium, and were cleaned in hydrofluoric acid before the contents were removed. Small amounts of CaF_2 remaining on the exterior of the capsules, even after cleaning, may have been incorporated into the starting material used in the crystallization experiments during extraction and grinding of this glassy material. Therefore, Ca contents were measured in all experiments to check for possible CaF_2 contamination. Minor amounts of CaO (≤0.3 wt%) were measured in melts from some of the crystallization experiments. This probably represents contamination from residual CaF_2 present on the exterior of the capsule used to prepare the high-T glass-rich starting materials.

Experimental products were removed from the capsule, mounted in epoxy resin, and polished. Electron microprobe analyses of the phases present were obtained using a JEOL JXA-8600 superprobe with a sample current of 5 nA and an accelerating potential of 15 kV. F was analyzed with a JEOL LDE1 multilayer crystal, using both synthetic F-rich phlogopite and natural topaz standards. Results obtained from both standards were within the uncertainties of counting statistics. Other elements were analyzed using either synthetic or natural minerals as standards (Si: natural quartz, Al and Ca: synthetic anorthite, K: synthetic orthoclase, Mg: synthetic spinel, Ti: synthetic rutile, Fe: natural fayalite, and Na: natural albite). X-ray intensities were reduced by means of a PRZ correction routine. Analyses were performed with the beam in rastering mode at magnifications between 60000 and 90000. This method was used to limit migration of light elements during the analyses and to insure accurate targeting. No decay of K count rates occurs at these analytical conditions (Patiño Douce and Beard 1995). In some cases, grain size was too small to obtain uncontaminated analyses, which is demonstrated by high SiO_2 con-

TABLE 3.—*Continued*

Expt.	DD38	DD14*	DD42	APD616	DD44	DD30	DD20*	DD52	DD53	DD54
P (kbar)	10	10	10	10	10	10	15	15	15	15
T (°C)	1250	1263	1275	1275	1290	1300	1300	1300	1300	1313
n**	6	6	6	3	4	3	9	6	7	3
					wt% oxides					
SiO_2	46.35	43.04	44.24	41.99	44.37	44.52	42.55	44.10	43.95	43.79
Al_2O_3	12.42	12.40	12.46	13.29	11.92	11.88	12.40	11.93	13.03	13.15
TiO_2	3.05	2.28	2.39	0.79	2.13	2.17	2.10	2.41	2.94	3.09
FeO†	0.10	0.27	0.04	0.82	0.05	0.39	0.62	0.14	0.16	0.15
MgO	23.93	25.79	26.11	26.68	25.97	26.31	25.47	24.98	25.89	26.12
Na_2O	0.17	0.13	0.18	0.12	0.12	0.09	0.14	0.08	0.19	0.07
K_2O	9.59	10.50	10.08	10.66	10.26	10.05	10.73	10.60	10.56	10.64
F	6.57	8.68	7.68	8.14	8.35	7.73	7.96	7.31	7.57	8.40
Oxide total	102.18	103.09	103.16	102.51	103.17	103.14	101.97	101.55	104.28	105.41
$-O \equiv F$	2.77	3.65	3.23	3.43	3.52	3.25	3.35	3.08	3.19	3.54
Total	99.41	99.44	99.93	99.08	99.65	99.89	98.62	98.47	101.09	101.87
					Stoichiometries based on O = 11					
Si	3.16	3.02	3.07	3.00	3.08	3.07	3.01	3.09	3.00	2.99
$^{[4]}Al$	0.84	0.98	0.93	1.00	0.92	0.93	0.99	0.91	1.00	1.01
$^{[6]}Al$	0.16	0.04	0.04	0.04	0.06	0.04	0.04	0.07	0.05	0.04
Mg	2.43	2.70	2.71	2.80	2.69	2.71	2.68	2.61	2.64	2.65
Ti	0.16	0.12	0.12	0.06	0.11	0.11	0.11	0.13	0.15	0.16
Fe	0.01	0.02	0.01	0.05	0.00	0.02	0.04	0.01	0.01	0.01
K	0.83	0.94	0.86	0.96	0.91	0.89	0.97	0.95	0.92	0.93
Na	0.02	0.02	0.04	0.01	0.02	0.01	0.02	0.01	0.03	0.01
F	1.42	1.92	1.66	1.81	1.83	1.69	1.78	1.62	1.64	1.81
OH	0.58	0.08	0.34	0.19	0.17	0.31	0.22	0.38	0.36	0.19
F/(F + OH)	0.71	0.96	0.83	0.91	0.92	0.84	0.89	0.81	0.82	0.91

TABLE 4. Melt compositions

Expt.	DD19*	DD39	DD29	DD45	DD50	DD27	DD33	DD40	APD612	DD13*	DD38	DD14*	DD42
P (kbar)	7	7	7	7	7	7	7	7	10	10	10	10	10
T (°C)	1250	1250	1275	1275	1290	1300	1375	1375	1075	1150	1250	1263	1275
n**	7	5	12	5	7	6	6	7	1	7	4	14	6
						wt% oxides							
SiO_2	76.03	71.41	73.52	72.69	71.73	72.26	67.13	70.08	71.28	72.74	71.39	73.73	70.30
Al_2O_3	9.31	11.74	10.73	10.70	10.57	10.86	9.19	9.62	10.54	12.34	12.95	11.75	13.41
TiO_2	2.04	2.84	3.32	3.19	3.75	3.45	5.18	4.81	0.63	0.86	2.54	2.57	2.58
FeO†	0.73	0.02	0.06	0.06	0.04	0.13	1.07	1.16	0.08	0.41	0.02	0.29	0.04
MgO	3.38	4.68	3.88	4.41	5.76	5.67	10.25	6.28	2.31	3.35	4.21	3.40	4.49
CaO	0.04	0.31	0.10	0.30	0.23	0.18	0.07	0.06	0.05	0.05	0.25	0.05	0.24
Na_2O	0.31	0.35	0.29	0.33	0.31	0.18	0.19	0.20	0.47	0.43	0.47	0.22	0.68
K_2O	7.11	6.23	7.10	6.60	6.48	6.88	5.48	6.15	7.07	7.71	7.45	6.91	6.95
F	1.27	2.09	2.27	2.42	2.55	2.37	2.49	2.69	0.71	0.98	1.10	2.11	1.95
Oxide total	100.22	99.65	101.25	100.69	101.42	101.98	101.03	101.03	93.14	98.86	100.38	101.02	100.65
$-O \equiv F$	0.53	0.88	0.95	1.02	1.07	1.00	1.05	1.13	0.30	0.41	0.46	0.89	0.82
Total	99.69	98.77	100.30	99.68	100.35	100.98	99.98	99.90	92.84	98.45	99.92	100.14	99.83
						$Al_2O_3/CaO + Na_2O + K_2O$ (molar)							
A/CNK	1.12	1.49	1.29	1.30	1.40	1.40	1.47	1.38	1.25	1.35	1.39	1.48	1.48

Note: Relative uncertainties of the average values (two standard deviations) are 2% for SiO_2, 5% for Al_2O_3, 6% for K_2O, 11% for TiO_2, 17% for F, 24% for MgO, 31% for Na_2O, and 42% for CaO.

* Experiments performed with mixture FTi-1.

** The number of melt pools analyzed per experiment.

† Total Fe reported as FeO.

tents reported for some grains of the phlogopite analyzed (Table 3).

Most analytical totals for hydrous phases, phlogopite, and melt are close to 100 wt% and, in a few cases, exceed 100 wt% even after the O equivalent of the F atoms is subtracted (see Tables 3 and 4). Therefore, it is impossible to estimate H_2O contents of these phases by difference. Calculated phlogopite stoichiometries (Table 3) suggest that phlogopite at $T > 1200$ °C may be essentially anhydrous, and so most of the H_2O would be dissolved in the melt. However, estimation of H_2O of the glasses by mass balance is not warranted given the potentially high permeability of silver palladium alloy to H_2 (Holloway and Wood 1988, p. 174) and perhaps even to H_2O (cf. Patiño Douce and Beard 1994). H_2O contents in the experimental products, therefore, remain unknown. This uncertainty does not invalidate the phase-equilibrium results, which describe the behavior of F- and Ti-rich phlogopite + quartz under strongly H_2O-undersaturated conditions (bulk $H_2O \leq 1$ wt%). In particular, conclusions about (1) F-Ti interactions in phlogopite, (2) the effects of these components on phlogopite stability, and (3) melt compositions produced in F-rich systems are unaffected. No conclusions can be drawn from our results, however, about the efficacy of Ti- and F-rich phlogopite as an H_2O reservoir at high temperatures.

Approach to equilibrium

Experimental durations were brief to minimize desiccation of the experimental samples with time as a result of either H_2 (Holloway and Wood 1988) or H_2O diffusion (Patiño Douce and Beard 1994) through the capsule material. Crystallization of phlogopite and quartz from the glassy starting material, at the same P and T at which these phases were present in melting experiments, suggests that a good approach to equilibrium was attained in the melting experiments, even if their durations were short (Table 1). The stability of the phase assemblages observed in the short-duration experiments was also verified by performing two longer duration experiments near the melt-in and Phlogopite-out phase boundaries at 10 kbar. The assemblage and modal proportions of the phases present in these longer duration experiments were the same as those observed in the shorter duration experiments (see Table 1). Phlogopite present in the longer duration experiments is similar in composition to that contained in the shorter duration experiments at the same P and T, with the exception of F content, which is higher in the longer duration experiments (Table 3). This observation suggests that H_2 (or H_2O) loss does indeed occur during the experiments. As a result of increased H_2 loss, H_2O loss, or both, the thermal stability of phlogopite could be artificially extended. Therefore, short experimental durations (with convergence of results from melting and crystallization experiments) minimize the possibility of overestimating phlogopite stability.

EXPERIMENTAL RESULTS

Description of phases

Phlogopite. In the melting experiments phlogopite occurs as euhedral crystals forming thin plates (3 μm thick, 10–60 μm across) at $T < 1075$ °C. As temperature increases, the crystal width increases to ~8 μm. Phlogopite present in the crystallization experiments is also euhedral but is finer grained. The high silica contents reported for phlogopite in some crystallization experiments may reflect contamination by glass surrounding smaller grains.

Pyroxene. It is not known whether the Mg-rich, Ca-

TABLE 4.—*Continued*

Expt.	APD616	DD44	DD30	DD34	DD35	DD31	DD20*	DD52	DD53	DD54	DD48	DD51	DD46	DD32
P (kbar)	10	10	10	10	10	10	15	15	15	15	15	15	15	15
T (°C)	1275	1290	1300	1300	1325	1350	1300	1300	1300	1313	1325	1350	1363	1400
*n***	3	7	10	8	6	3	8	8	3	7	8	7	4	3
							wt% oxides							
SiO_2	72.30	71.94	73.45	69.69	70.88	69.92	72.97	71.74	69.14	69.64	67.68	69.18	68.80	67.69
Al_2O_3	11.99	12.03	11.04	12.05	10.29	9.68	11.14	12.01	13.09	14.58	11.96	11.06	11.54	10.63
TiO_2	2.54	2.44	2.72	3.43	4.28	5.01	2.39	2.56	2.32	1.94	4.30	3.68	3.45	5.71
FeO†	0.40	0.05	0.25	0.01	0.03	0.03	0.48	0.20	0.03	0.04	0.00	0.05	0.06	0.04
MgO	3.45	4.46	4.03	5.81	5.95	7.42	2.94	3.61	4.68	3.06	6.40	4.82	5.51	8.19
CaO	0.10	0.30	0.10	0.17	0.09	0.05	0.03	0.09	0.50	0.52	0.07	0.08	0.24	0.05
Na_2O	0.31	0.47	0.29	0.18	0.13	0.24	0.46	0.27	0.57	0.44	0.23	0.22	0.35	0.23
K_2O	7.70	7.38	6.99	7.16	6.97	6.66	8.97	8.03	8.18	8.64	7.82	7.84	7.72	7.29
F	2.23	2.03	2.03	2.30	2.22	2.69	1.90	2.00	1.65	1.62	2.95	2.93	2.69	2.89
Oxide total	101.02	101.05	100.90	100.81	100.83	101.69	101.27	100.51	100.15	100.48	101.42	99.87	100.37	102.72
−O ≡ F	0.94	0.85	0.86	0.97	0.93	1.13	0.80	0.84	0.69	0.68	1.24	1.23	1.13	1.22
Total	100.08	100.20	100.05	99.84	99.90	100.56	100.47	99.67	99.45	99.80	100.17	98.64	99.23	101.51
							$Al_2O_3/CaO + Na_2O + K_2O$ (molar)							
A/CNK	1.36	1.29	1.34	1.44	1.33	1.26	1.06	1.31	1.50	1.60	1.49	1.37	1.43	1.41

free pyroxene crystals observed in the experimental products are monoclinic or orthorhombic; therefore, they are referred to simply as pyroxene. In all experiments pyroxene occurs as thin needles to blade-like crystals, <5 μm wide and ~10–15 μm long. The grain size of pyroxene increases with temperature to 10 μm wide and 30 μm long. The pyroxene crystals contain substantial amounts of Al, thus they are not end-member enstatite. Al concentrations in pyroxene vary from ~0.6 wt% at 7 kbar and 1375 °C to 8.1 wt% Al_3O_2 at 10 kbar and 1150 °C (Table 5). Pyroxene grains are not compositionally zoned; the apparent zoning shown in Figure 1 results from the positive relief of pyroxene relative to the surrounding material caused by polishing.

Rutile. Rutile occurs as subhedral to anhedral grains ranging in size from 1 to 10 μm.

Quartz. Quartz occurs as globular, anhedral grains, 5–30 μm in diameter.

Melt. Melt is abundant in all experiments at $T > 1200$ °C. It forms a continuous matrix in which mineral phases are dispersed (Fig. 1). In near-solidus experiments at 7 and 10 kbar melt is present in minor amounts, but no well-developed melt pools are present. Therefore, melt is difficult to identify and to analyze.

TABLE 5. Representative pyroxene compositions

Expt.	DD19*	DD50	DD33	DD11*	DD13*	DD35	DD52	DD48	DD46
P (kbar)	7	7	7	10	10	10	15	15	15
T (°C)	1250	1290	1375	1050	1150	1325	1300	1325	1363
*n***	4	4	4	4	4	5	5	6	2
					wt% oxides				
SiO_2	59.62	58.40	59.27	54.47	57.89	58.80	58.61	58.30	59.05
Al_2O_3	2.15	1.19	0.63	7.22	8.21	0.98	1.38	1.63	1.48
TiO_2	0.80	0.89	0.62	0.45	0.65	0.84	0.58	0.78	0.66
FeO†	3.68	2.27	1.92	5.91	3.82	1.58	2.34	1.24	0.93
MgO	32.60	37.83	38.22	31.05	29.83	37.80	37.07	37.10	38.24
Total	98.86	100.58	100.65	99.11	100.41	100.00	99.98	99.05	100.37
					Stoichiometries based on O = 6				
Si	2.03	1.96	1.98	1.88	1.94	1.98	1.98	1.98	1.97
$^{[4]}Al$	0.00	0.04	0.02	0.12	0.06	0.02	0.02	0.02	0.03
$^{[6]}Al$	0.09	0.01	0.01	0.18	0.27	0.02	0.03	0.04	0.03
Ti	0.02	0.02	0.02	0.01	0.02	0.02	0.01	0.02	0.02
Fe	0.10	0.06	0.05	0.17	0.11	0.04	0.07	0.04	0.03
Mg	1.66	1.90	1.91	1.60	1.49	1.90	1.87	1.87	1.91
Total	3.90	3.99	3.99	3.96	3.88	3.98	3.98	3.97	3.98

Note: Relative uncertainties of the average values (two standard deviations) are 2% for SiO_2, 4% for MgO, 20% for FeO, 24% for TiO_2, and 28% for Al_2O_3.

* Experiments performed with mixture FTi-1.

** The number of grains analyzed per experiment.

† Total Fe reported as FeO.

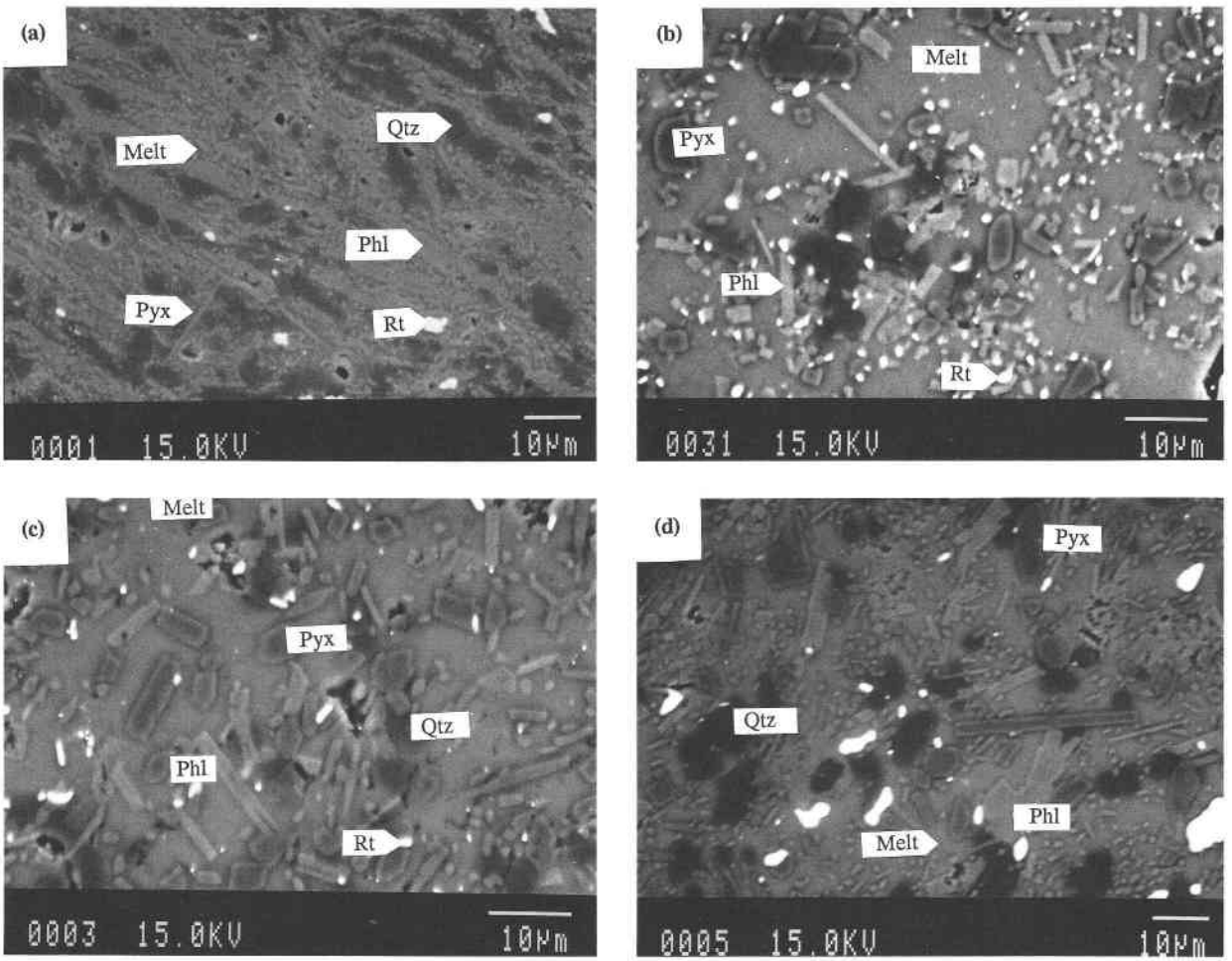

FIGURE 1. Backscattered electron images. (**a**) Melting experiment with minor amounts of melt at 10 kbar, 1150 °C; (**b**) crystallization experiment at 7 kbar, 1250 °C; (**c**) crystallization experiment at 10 kbar, 1290 °C; and (**d**) melting experiment at 15 kbar, 1300 °C. Note the smaller grain size of phlogopite from crystallization experiments.

Phase relations

Phase relations determined in this study are summarized in Figure 2. The solidus of the assemblage F-rich phlogopite + quartz + rutile was approached at 7 and 10 kbar (Table 1). At 7 kbar, 1038 °C and 10 kbar, 1050 °C, trace amounts of pyroxene were observed but no melt was positively identified. Pyroxene may form below the solidus by melt- and fluid-absent reactions involving Ti-Fe or Ti-Mg exchange components in mica such as

$$TiO_2 + 2SiO_2 \rightleftharpoons (TiMg_{-2})_{Phl} + 2MgSiO_3$$

(Patiño Douce 1993; Patiño Douce and Beard 1995). However, phlogopite in these experiments is enriched in F relative to that in the starting mixture, suggesting that some phlogopite may have reacted, yielding a hydrous melt that we were unable to detect. Melt was positively identified at 7 kbar, 1050 °C and 10 kbar, 1075 °C (at the latter conditions, after both 52 and 172 h). The degree of melting observed in both the short- and long-duration experiments at 10 kbar and 1075 °C is very low (see Table 1).

The upper thermal stability of Ti- and F-rich phlogopite in the assemblage F-rich phlogopite + quartz + rutile was bracketed by means of melting and crystallization experiments (Fig. 2). The phlogopite-out boundary at 7 kbar is bracketed between 1275 and 1290 °C. At 7 kbar quartz disappears at a temperature between 1300 and 1375 °C, and rutile is near its upper stability limit at 1375 °C, as determined from the results of the two melting experiments performed at these conditions, one of which contained only minor amounts of rutile (Table 1). At 10 kbar, the assemblage F-rich phlogopite + melt + pyroxene + quartz + rutile is present over the temperature interval 1075–1295 °C. At temperatures above 1295 °C at 10 kbar phlogopite is no longer present. The solidus temperature was not determined at 15 kbar, but the phlogopite-out boundary lies between 1313 and 1325 °C.

The terminal reaction for Ti- and F-rich phlogopite in the bulk compositions that we studied has a slope of ~220

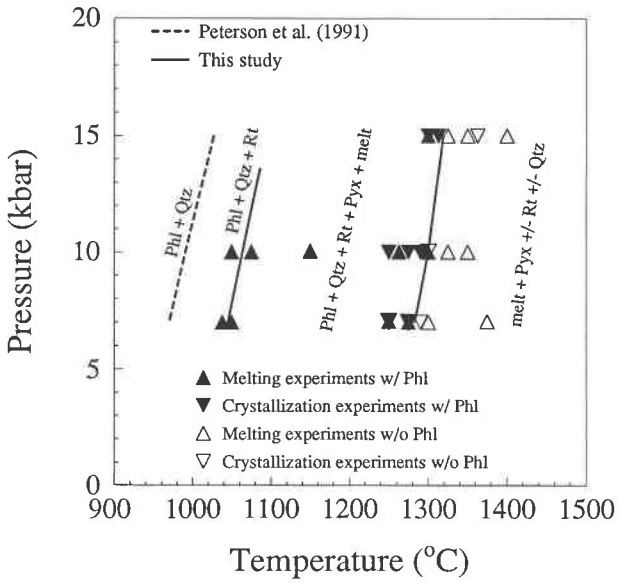

FIGURE 2. *P-T* phase relations as determined by this experimental study. The assemblage Phl + Qtz + melt + Rt + Pyx is stable over a temperature interval of more than 200 °C. The Phl-out boundary is approximately 300 °C higher at 10 kbar for Ti-saturated experiments (this study) in comparison with the same Ti-free assemblage (Peterson et al. 1991).

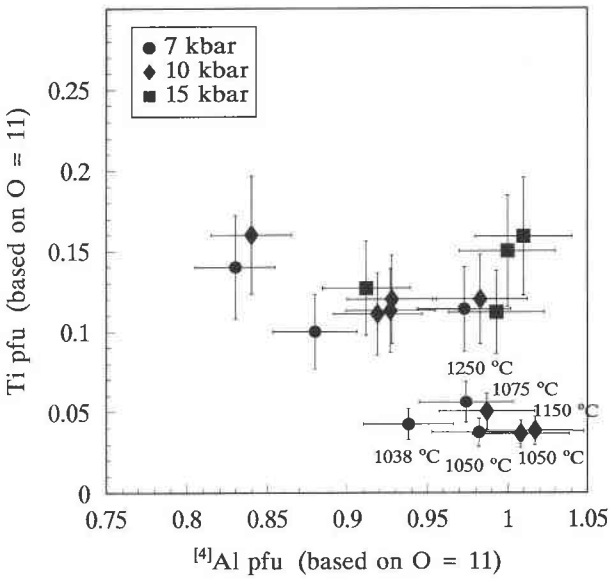

FIGURE 3. Ti pfu vs. $^{[4]}$Al pfu, suggesting that the Ti-Tschermak's substitutional mechanism ($Ti^{[4]}Al_2Mg_{-1}Si_{-2}$) does not occur in the phlogopite from these experiments. Data points not labeled with a temperature are for experiments performed at $T \geq 1250$ °C.

bars/°C, although the slope apparently steepens between 10 and 15 kbar. At 10 kbar our Ti- and F-rich phlogopite-out boundary is approximately 450 °C higher than that reported for the KMASH system (Bohlen et al. 1983; Peterson and Newton 1989; Vielzeuf and Clemens 1992) and 300 °C higher than that for the F-KMASH system (Peterson et al. 1991, Fig. 2). Note that the phlogopite-out boundary was tightly bracketed at 7, 10, and 15 kbar by the overlap of melting and crystallization experiments (Table 1, Fig. 2).

Phlogopite compositions

Although Ti contents increased in the experimental products relative to the starting phlogopite composition (Table 3), there are no systematic variations of Ti content with either pressure or temperature. However, Ti contents in phlogopite are low in comparison with those found in other experimental studies with more Fe-rich and F-poor biotite (e.g., Patiño Douce and Johnston 1991; Patiño Douce et al. 1993; Patiño Douce and Beard 1995) and also in comparison with biotite from granulite-facies rocks (e.g., Guidotti 1984). For example, phlogopite in our experiments contains 8.0 wt% F near the phlogopite-out boundary at 7, 10, and 15 kbar, but TiO_2 contents are ~2–3 wt% (cf. Table 3). There may be several reasons for the low Ti concentrations in these phlogopite compositions.

Possible mechanisms of Ti substitution in phlogopite and biotite are the Ti-vacancy ($Ti\square R^{2+}_{-2}$), Ti-Tschermak's ($TiAl_2R^{2+}_{-1}Si_{-2}$), and Ti-oxy [$TiO^{2-}_2R^{2+}_{-1}(OH)^{-}_{-2}$], where R represents Fe^{2+} or Mg^{2+} (e.g., Abrecht and Hewitt 1988). These proposed substitutional mechanisms suggest that the concentrations of Fe^{2+}, Mg, Al, Si, and OH^- may significantly affect Ti concentration in phlogopite. End-member phlogopite described in the experimental studies performed by Trønnes et al. (1985), Robert (1976), and Abrecht and Hewitt (1988) contains substantially more Ti than the phlogopite in this study. Results of these earlier experimental studies, therefore, rule out low Fe concentrations as a limiting factor on Ti concentration. The amount of Ti that enters phlogopite may also be partially controlled by Al content through the incorporation of the Ti-Tschermak's exchange. The phlogopite crystals present in our experiments do not contain substantial amounts of excess Al. However, for Al-poor phlogopite, it appears unnecessary to incorporate a Ti-Tschermak's component in phlogopite to achieve Ti concentrations greater than those observed here (Abrecht and Hewitt 1988). In addition, there is no clear correlation between Al and Ti concentration in the phlogopite crystals from these experiments (Fig. 3), as would be expected from the Ti-Tschermak's exchange.

F content may have a strong influence on Ti substitution in phlogopite, as is the case with both Al and Fe (Munoz and Ludington 1974). Compositions of phlogopite in our high-temperature experiments (>1250 °C) suggest an inverse correlation between F and Ti contents (Fig. 4). Bohlen et al. (1980) concluded that it is necessary to include the Ti-oxy exchange component [$TiO^{2-}_2R^{2+}_{-1}\cdot(OH)^{-}_{-2}$], in addition to other Ti components, to describe fully the Ti substitutions that occur in biotite. The synthesis experiments of Abrecht and Hewitt (1988) confirm this conclusion for Mg-rich biotite and phlogopite. Charge

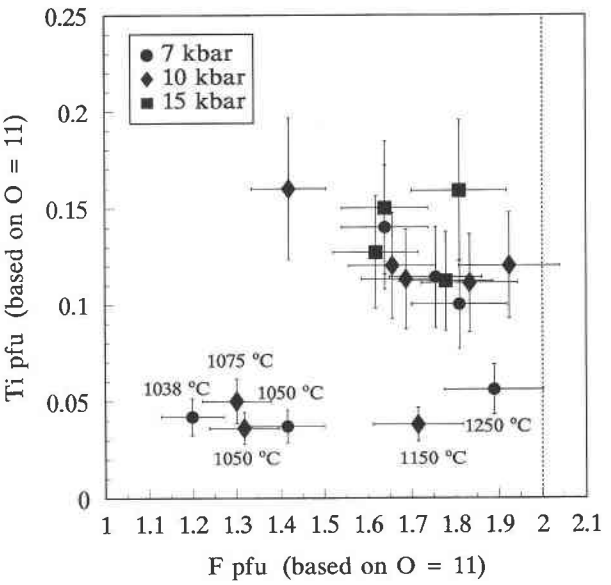

FIGURE 4. Ti pfu vs. F pfu, showing a rough correlation between F and Ti contents. The decrease of Ti content with increasing F content indicates that either the lack of available OH^- groups or a Ti-F avoidance mechanism inhibits the amount of Ti that can enter phlogopite. Data points not labeled with a temperature are for experiments performed at $T \geq 1250$ °C.

balance in the mica structure is maintained by increasing the negative charge from OH^- to O^{2-} when a highly charged cation such as Ti^{4+} is incorporated. Therefore, operation of the Ti-oxy substitution requires available OH^- groups to exchange with O^{2-}. Because F substitutes into the phlogopite structure by exchanging F^- with OH^- (e.g., Munoz 1984), a possible interpretation of our experimental observations (Fig. 4) is that the Ti-oxy substitution is hampered as the availability of OH^- groups decreases with increasing F content. Lower temperature ($T \leq 1150$ °C) phlogopite that does not fall on the main trend (Fig. 4) contains much less TiO_2 than would be expected, in comparison with the high-temperature phlogopite, and coexists with only minor amounts of melt (or none at all). This lower temperature phlogopite may not represent equilibrium compositions.

Despite the fact that the solubility of Ti in F-rich phlogopite is limited, our results show that these relatively low Ti concentrations are sufficient to cause a dramatic increase in the thermal stability of the assemblage F-rich phlogopite + quartz. This is demonstrated by comparing the results of our study with those of Peterson et al. (1991). Figure 2 shows that the phlogopite-out boundary of the rutile-bearing assemblage is located at a temperature 300 °C higher than that of the equivalent Ti-free assemblage.

Melt compositions

Melt compositions are strongly peraluminous and silica rich, with SiO_2 contents between 67 and 76 wt% and molar $Al_2O_3/(K_2O + Na_2O + CaO)$ ratios in the range 1.1–1.6 (Table 4). The differences in melt compositions observed in melting and crystallization experiments containing the same phase assemblage and performed at the same P and T are relatively minor (Table 4). These melt compositions are very different from those of the lamproitic melts reported by Peterson et al. (1991) for dehydration melting in the F-KMASH system. The melt compositions observed in our experiments are granitic, such as those reported by Vielzeuf and Clemens (1992) for fluid-absent melting in the KMASH system. The melt compositions observed in this study are also similar in SiO_2 contents and molar $Al_2O_3/(K_2O + Na_2O + CaO)$ ratios to melts generated by fluid-absent melting of an F-rich tonalitic gneiss reported by Skjerlie and Johnston (1993). Mg contents observed in our experiments are elevated relative to typical peraluminous granites. This was expected given the high temperatures of our experiments. The strongly peraluminous character of the melts may be attributed, at least in part, to their high F contents, which increase Al solubility in silicate melts (Manning et al. 1980). These authors have shown that increased F drives melts in the quartz-albite-orthoclase system toward more peraluminous compositions, and our results are in agreement with this conclusion.

The difference between melt compositions reported by Peterson et al. (1991) for melting of F-rich phlogopite + quartz and melt compositions determined in this study is striking and requires an explanation. Peterson et al. (1991) did not mention whether the glass analyses were obtained from polished sections, but the analyses of glass from a single experimental product show large compositional variations, suggesting that they may represent contaminated glass analyses (i.e., other phases may have been included in the analyses). In contrast, melt compositions were determined in this study from numerous replicate analyses (Table 4) of polished sections. The melt compositions observed in our experiments are restricted to a narrow compositional range (Table 4), even if melt compositions were not strictly reversed in paired melting and crystallization experiments performed at the same P and T and with the same starting mixture (FTi-2). This difference in analytical techniques may explain the discrepancy between the melt compositions reported by Peterson et al. (1991) and those found in our experiments because the only other difference between our experiments and those of Peterson et al. (1991) is the presence of rutile. Ti saturation should not have a strong effect on melt compositions, given the relatively low solubility of Ti in silicic melts (cf. Table 4). Our results thus show that fluid-absent melting of phlogopite in F-rich, quartz-saturated assemblages generates melts of granitic composition, rather than lamproites as suggested by Peterson et al. (1991).

DISCUSSION AND GEOLOGIC IMPLICATIONS

Phlogopite stability

The strong effects of both F and Ti on the thermal stability of micas have been previously documented (e.g.,

Valley et al. 1982; Munoz 1984; Trønnes et al. 1985; Patiño Douce 1993). This study indicates that the two components in combination increase the thermal stability of phlogopite to a much greater extent than either component independently. F- and Ti-rich phlogopite could thus be an important reservoir for K and large-ion lithophile elements at great depths in the crust and upper mantle. Whether F- and Ti-rich phlogopite can be an important H_2O reservoir in the deep lithosphere, however, remains unknown.

The behavior of phlogopite in these experiments suggests that in Mg-rich micas the Ti substitution mechanism at high T may be controlled, to a large extent, by the availability of OH^- groups. The Ti-oxy substitution mechanism has been shown to be important for Mg-rich biotite (Abrecht and Hewitt 1988), and F^- enters the phlogopite structure by replacing OH^-. Low Ti solubility in F-rich phlogopite is consistent with operation of both the F^-OH_{-1} and Ti-oxy substitution mechanisms.

Implications for the origin of A-type granites

Our experiments demonstrate that fluid-absent melting of the assemblage Ti- and F-rich phlogopite + quartz at very high temperatures yields granitic peraluminous melts. A-type granites have often been characterized as high-T melts containing substantial amounts of alkalis and F and relatively little H_2O (White and Chappell 1983; Whalen et al. 1987). A-type granites commonly vary in composition from peralkaline to metaluminous and are rarely peraluminous (Collins et al. 1982; Eby 1990). One hypothesis for the origin of metaluminous A-type granites is that they formed by high-T, fluid-absent melting of a previously melt-depleted lower crustal source containing halogen-enriched micas and amphiboles (Collins et al. 1982; Clemens et al. 1986). Our results, in agreement with the earlier work of Manning et al. (1980), show that melts derived from fluid-absent melting of protoliths containing halogen-enriched micas are strongly peraluminous and are not likely to resemble the majority of A-type granites.

Conclusions

The thermal stability of the assemblage Ti- and F-rich phlogopite + quartz + rutile, with F-rich phlogopite containing 0.2 Ti atoms pfu, is approximately 300 °C higher than that of the equivalent Ti-free assemblage at the same pressure. This shows the large combined effect of Ti and F in extending the thermal stability of phlogopite. Peterson et al. (1991) demonstrated that high F content alone increases the thermal stability of phlogopite + quartz. Solution of even a relatively small amount of TiO_2 ($\approx$2 wt%) enhances the thermal stability of F-rich phlogopite dramatically. To discriminate completely the individual effects of Ti and F on phlogopite stability, however, it would be necessary to conduct similar experiments with the F-free assemblage Ti-rich phlogopite + quartz + rutile.

Our results also show that granitic melts derived from fluid-absent melting of crustal protoliths containing halogen-enriched micas are likely to be strongly peraluminous. This suggests that peralkaline and metaluminous A-type granites are not likely to be primary melts of halogen-enriched crustal protoliths. In contrast, strongly peraluminous and F-rich topaz rhyolites (Burt et al. 1982) and ongonites (Kovalenko et al. 1977) could represent such near primary melts.

Acknowledgments

We thank J. Clemens and R. Wendlandt for their helpful reviews of this manuscript. This study was funded by NSF grants EAR-9118418 and EAR-9316304 to A.E.P.D. Electron microprobe analyses were performed at the University of Georgia. The microprobe was acquired with NSF grant EAR-8816748 and a matching grant from the University of Georgia Research Foundation.

References cited

Abrecht, J., and Hewitt, D.A. (1988) Experimental evidence on the substitution of Ti in biotite. American Mineralogist, 73, 1275–1284.

Aoki, K., Ishiwaka, K., and Kanisawa, S. (1981) Fluorine geochemistry of basaltic rocks from continental and oceanic regions and petrogenetic application. Contributions to Mineralogy and Petrology, 76, 53–59.

Bohlen, S.R., Peacor, D.R., and Essene, E.J. (1980) Crystal chemistry of a metamorphic biotite and its significance in water barometry. American Mineralogist, 65, 55–62.

Bohlen, S.R., Boettcher, A.L., Wall, V.J., and Clemens, J.D. (1983) Stability of phlogopite-quartz and sanidine-quartz: A model for melting in the lower crust. Contributions to Mineralogy and Petrology, 83, 270–277.

Burt, D.M., Sheridan, M.F., Bikun, J.V., and Christiansen, E.H. (1982) Topaz rhyolites: Distribution, origin, and significance for exploration. Economic Geology, 77, 1818–1836.

Chacko, T., Ravindra Kumar, G.R., and Newton, R.C. (1987) Metamorphic P-T conditions of the Kerala (South India) khondalite belt, a granulite facies supracrustal terrain. Journal of Geology, 95, 343–358.

Clemens, J.D., Holloway, J.R., and White, A.J.R. (1986) Origin of an A-type granite: Experimental constraints. American Mineralogist, 71, 317–324.

Collins, W.J., Beams, S.D., White, A.J.R., and Chappell, B.W. (1982) Nature and origin of A-type granites with particular reference to southeastern Australia. Contributions to Mineralogy and Petrology, 80, 189–200.

Dymek, R.F. (1983) Titanium, aluminum and interlayer cation substitutions in biotite from high-grade gneisses, West Greenland. American Mineralogist, 68, 880–899.

Eby, G.N. (1990) The A-type granitoids: A review of their occurrence and chemical characteristics and speculation on their petrogenesis. Lithos, 26, 115–134.

Guidotti, C.V. (1984) Micas in metamorphic rocks. In Mineralogical Society of America Reviews in Mineralogy, 13, 357–476.

Holloway, J.R., and Wood, B.J., Eds. (1988) Simulating the Earth, 196 p. Unwin Hyman, Boston.

Kovalenko, V.I., Antipin, V.S., Konusova, V.V., Smirnova, Ye. V., Petrov, L.L., Vladykin, N.V., Kuznetsova, A.I., Kostyukova, Ye.S., and Pisarskaya, V.A. (1977) Partition coefficients of fluorine, niobium, tantalum, lanthanum, ytterbium, yttrium, tin and tungsten in ongonite. Doklady Earth Science Section, 233, 203–205.

Kretz, R. (1983) Symbols for rock-forming minerals. American Mineralogist, 68, 277–279.

Leelanandam, C. (1969) H_2O^+, F and Cl in the charnockitic biotites from Kondapalli, India. Neues Jahrbuch für Mineralogie Monatshefte, 10, 461–468.

Manning, D.A.C., Hamilton, D.L., Henderson, C.M.B., and Dempsey, M.J. (1980) The probable occurrence of interstitial Al in hydrous, F-bearing and F-free aluminosilicate melts. Contributions to Mineralogy and Petrology, 75, 257–262.

Modreski, P.J., and Boettcher, A.L. (1972) The stability of phlogopite and

enstatite at high pressures: A model for micas in the interior of the Earth. American Journal of Science, 272, 852–869.

——— (1973) Phase relationships of phlogopite in the system K_2O-MgO-CaO-Al_2O_3-SiO_2-H_2O to 35 kilobars: A better model for micas in the interior of the Earth. American Journal of Science, 273, 385–414.

Monier, G., and Robert, J.L. (1986) Titanium in muscovites from two mica granites: Substitutional mechanism and partition with coexisting biotites. Neues Jahrbuch für Mineralogie Abhandlungen, 153(2), 147–161.

Munoz, J.L. (1984) F-OH and Cl-OH exchange in micas with applications to hydrothermal ore deposits. In Mineralogical Society of America Reviews in Mineralogy, 13, 357–476.

Munoz, J.L., and Ludington, S. (1974) Fluorine-hydroxyl exchange in biotite. American Journal Science, 274, 396–413.

——— (1977) Fluorine-hydroxyl exchange in synthetic muscovite and its application to muscovite-biotite assemblages. American Mineralogist, 62, 304–308.

Patiño Douce, A.E. (1993) Titanium substitution in biotite: An empirical model with applications to thermometry, O_2 and H_2O barometries, and consequences for biotite stability. Chemical Geology, 108, 133–162.

——— (1995) Experimental generation of hybrid silicic melts by reaction of high-Al basalts with metamorphic rocks. Journal of Geophysical Research, 100, 15623–15639.

Patiño Douce, A.E., and Johnston, A.D. (1991) Phase equilibria and melt productivity in the pelitic system: Implications for the origin of peraluminous granitoids and aluminous granulites. Contributions to Mineralogy and Petrology, 107, 202–218.

Patiño Douce, A.E., Johnston, A.D., and Rice, J.M. (1993) Octahedral excess mixing properties in biotite: A working model with applications to geobarometry and geothermometry. American Mineralogist, 78, 113–131.

Patiño Douce, A.E., and Beard, J.S. (1994) H_2O loss from hydrous melts during fluid-absent piston cylinder experiments. American Mineralogist, 79, 585–588.

——— (1995) Dehydration-melting of biotite gneiss and quartz amphibolite from 3 to 15 kbar. Journal of Petrology, 36, 707–738.

Petersen, E.U., Essene, E.J., Peacor, D.R., and Valley, J.W. (1982) Fluorine end-member micas and amphiboles. American Mineralogist, 67, 538–544.

Peterson, J.W., and Newton, R.C. (1989) Reversed experiments on biotite-quartz-feldspar melting in the system KMASH: Implications for crustal anatexis. Journal of Geology, 97, 465–485.

Peterson, J.W., Chacko, T., and Kuehner, S.M. (1991) The effects of fluorine on the vapor-absent melting of phlogopite + quartz: Implications for deep-crustal processes. American Mineralogist, 76, 470–476.

Robert, J.L. (1976) Titanium solubility in synthetic phlogopite solid solutions. Chemical Geology, 17, 195–212.

Skjerlie, K.P., and Johnston, A.D. (1993) Fluid-absent melting behavior of an F-rich tonalitic gneiss at mid-crustal pressures: Implication for the generation of anorogenic granites. Journal of Petrology, 34, 785–815.

Thompson, A.B. (1982) Dehydration melting of pelitic rocks and the generation of H_2O-undersaturated granitic liquids. American Journal of Science, 282, 1567–1595.

Trønnes, R.G., Edgar, A.D., and Arima, M. (1985) A high pressure–high temperature study of TiO_2 solubility in Mg-rich phlogopites: Implication to phlogopite chemistry. Geochimica et Cosmochimica Acta, 49, 2323–2329.

Valley, J.W., Petersen, E.U., Essene, E.J., and Bowman, J.R. (1982) Fluorphlogopite and fluortremolite in Adirondack marbles and calculated C-O-H-F fluid compositions. American Mineralogist, 67, 545–557.

Vielzeuf, D., and Clemens, J.D. (1992) The fluid-absent melting of phlogopite + quartz: Experiments and models. American Mineralogist, 77, 1206–1222.

Wendlandt, R.F., and Eggler, D.H. (1980) The origin of potassic magmas: 2. Stability of phlogopite in natural spinel lherzolite and in the system $KAlSiO_4$-MgO-SiO_2-H_2O-CO_2 at high pressures and high temperatures. American Journal of Science, 280, 421–458.

Whalen, J.B., Currie, K.L., and Chappell, B.W. (1987) A-type granites: Geochemical characteristics, discrimination and petrogenesis. Contributions to Mineralogy and Petrology, 95, 407–419.

White, A.J.R., and Chappell, B.W. (1983) Granitoid types and their distribution in the Lachlan Fold Belt, southeastern Australia. Geological Society of America Memoir, 159, 21–34.

Wood, B.J. (1976) The reaction phlogopite + quartz = enstatite + sanidine + H_2O. Progress in Experimental Petrology, 6, 17–19.

Wyllie, P.J., and Sekine, T. (1982) The formation of mantle phlogopite in subduction zone hybridization. Contributions to Mineralogy and Petrology, 79, 375–380.

Manuscript received January 13, 1995
Manuscript accepted September 18, 1995